Role of Methionine 230 in Intramolecular Electron Transfer between the Oxyferryl Heme and Tryptophan 191 in Cytochrome *c* Peroxidase Compound II†

Rui-Qin Liu,‡ Mark A. Miller,*,§ Gye Won Han,§ Seung Hahm,‡ Lois Geren,‡ Sharon Hibdon,‡ Joseph Kraut,§ Bill Durham,‡ and Francis Millett*,‡

Department of Chemistry and Biochemistry, University of Arkansas, Fayetteville, Arkansas 72701, and Department of Chemistry, University of California at San Diego, La Jolla, California 92093

Received February 15, 1994; Revised Manuscript Received May 11, 1994®

ABSTRACT: The kinetics of electron transfer from cytochrome *c* (CC) to yeast cytochrome *c* peroxidase (CcP) compound I were studied by flash photolysis and stopped-flow spectroscopy. Flash photolysis studies employed horse CC derivatives labeled at specific lysine amino groups with (dicarboxybipyridine)bis-(bipyridine)ruthenium (Ru-CC). Initial electron transfer from Ru-CC reduced the indole radical on Trp-191 of CcP compound I [CMPI(IV,R•)], producing CMPII(IV,R). This reaction was biphasic for each of several Ru-CC derivatives, with rate constants which varied according to the position of the Ru label. For Ru-27-CC labeled at lysine 27, rate constants of 43 000 and 1600 s^{-1} were observed at pH 5.0 in 2 mM acetate. After reduction of the indole radical by Ru-CC, intramolecular electron transfer from Trp-191 to the oxyferryl heme in CMPII(IV,R) was observed, producing CMPII(III,R•). The rate constant and extent of this intramolecular electron transfer reaction were independent of both the protein concentration and the Ru-CC derivative employed. The rate constant decreased from 1100 s^{-1} at pH 5 to 550 s^{-1} at pH 6, while the extent of conversion of CMPII(IV,R) to CMPII(III,R•) decreased from 56% at pH 5 to 29% at pH 6. The reaction was not detected at pH 7.0 and above. The pH dependence of the rate and extent of this internal electron transfer reaction paralleled the pH dependence of the rate of bimolecular reduction of CMPII(IV,R) by native horse CC measured by stopped-flow spectroscopy at high ionic strength. The internal electron transfer reaction and the bimolecular reduction of CMPII(IV,R) were also affected in parallel by the substitution of Ile for Met-230. Although the initial reduction of the radical in CMPI(IV,R•) by Ru-CC was not affected, the conversion of CMPII(IV,R) to CMPII(III,R•) could not be detected in photolysis experiments employing the M230I enzyme. Stopped-flow experiments showed that the rate constants for bimolecular reduction of CMPII(IV,R) to CcP(III,R) by horse CC and yeast iso-1-CC were decreased 12-fold by the M230I mutation, even though this mutation had no effect on the initial bimolecular reduction of the radical in CMPI(IV,R•). Crystallographic studies of the M230I mutant ruled out changes in the position of Trp-191 as the basis for this effect, suggesting that the internal electron transfer reaction is influenced by the interaction of Met-230 with the indole radical. The results clearly demonstrate that the internal electron transfer reaction and bimolecular reduction of CMPII(IV,R) by CC are altered in parallel by both pH and the M230I mutation, suggesting that electron transfer from Trp-191 to the oxyferryl iron is an obligatory step in the reduction of CMPII(IV,R). This interpretation predicts that the two intermolecular one-electron transfer reactions that reduce CMPI(IV,R•) to CcP(III,R) each proceed via reduction of the Trp-191 radical by CC and is consistent with a mechanism that utilizes a single, unique electron transfer pathway.

Cytochrome *c* peroxidase catalyzes the reduction of hydrogen peroxide to water by two molecules of ferrocytochrome *c* (Yonetani, 1965; Kim et al., 1990). In the first step of the mechanism, the resting ferric state of cytochrome *c* peroxidase, CcP, is oxidized by hydrogen peroxide to CMPI, which contains an oxyferryl heme Fe(IV) and a radical on the indole ring of Trp-191 (Mauro et al., 1988; Sivaraja et al., 1989; Erman et al., 1989; Fishel et al., 1991). CMPI is reduced to CMPII by one molecule of ferrocytochrome *c* [CC(II)], followed by reduction of CMPII to CcP by a second molecule of CC(II). Two forms of CMPII were identified by Coulson et al. (1971), CMPII(IV,R) containing the oxyferryl heme Fe^{IV}=O, and CMPII(III,R•) containing the radical. Combined ESR and spectrophotometric studies demonstrated that addition of 1 equiv of ferrocyanide or CC(II) to CMPI led to nearly exclusive formation of CMPII(IV,R) at pH 7 and above. However, at pH 6 and below a mixture of CMPII(IV,R) and CMPII-(III,R•) was formed. Coulson et al. (1971) proposed two possible mechanisms to explain these results, the rapid equilibrium mechanism shown in Scheme 1, and the independent sites mechanism shown in Scheme 2.

Scheme 1

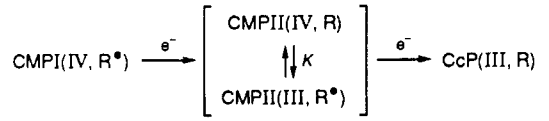

Scheme 2

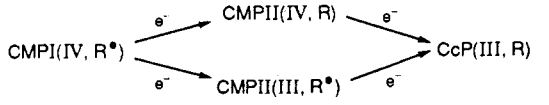

The equilibration between the two forms of CMPII in Scheme 1 is assumed to be rapid compared to the reduction

† This work was supported in part by NIH Grant NIH GM20488 to F.M. and B.D. and NSF Grant MCB 9119292 to J.K. and M.A.M.

‡ University of Arkansas.

§ University of California at San Diego.

® Abstract published in *Advance ACS Abstracts,* July 1, 1994.

0006-2960/94/0433-8678$04.50/0

Scheme 3

$$\text{CMPI(IV, R}^{\bullet}) + \text{CC(II)} \xrightarrow{k_1} \text{CMPII(IV, R)} + \text{CC(III)}$$

$$\text{CMPII(IV, R)} \underset{k_3}{\overset{k_2}{\rightleftharpoons}} \text{CMPII(III, R}^{\bullet})$$

$$\text{CMPII(III, R}^{\bullet}) + \text{CC(II)} \xrightarrow{k_4} \text{CcP(III, R)} + \text{CC(III)}$$

steps. The equilibrium constant K is less than 0.13 at pH 7 and above, but increases to 1.2 at pH 5 (Coulson et al., 1971). Ho et al. (1983) proposed that rapid electron transfer from Trp-191 to Fe^{IV}=O in CMPII occurs only in a transient conformation of the protein in which the redox potential of Trp-191 is decreased and the radical is stabilized: CMPII(IV,R) → CMPII(III,R•). The stable form of CMPII prepared by hydrogen peroxide oxidation of ferrous CcP, $CMPII(IV,R)_B$, is not rapidly converted to $CMPII(III,R^{\bullet})_B$ because the redox potential of R• is very high in this conformation of the protein.

Hahm et al. (1993, 1994) recently studied the reaction between horse cytochrome *c* (hCC) and CMPI using stopped-flow spectroscopy. CC(II) reduced the radical in CMPI to form CMPII(IV,R) with a second-order rate constant of 1.3×10^8 M^{-1} s^{-1} in 100 mM ionic strength buffer at pH 7. A second molecule of CC(II) then reduced CMPII(IV,R) to CcP(III,R) with a second-order rate constant of 9×10^6 M^{-1} s^{-1}. The rate constant for reduction of the radical was nearly independent of pH from 5 to 8, but the rate constant for reduction of the Fe^{IV}=O center increased 33-fold as the pH decreased from 8 to 5 (Hahm et al., 1994). This increase in rate was correlated with the pH dependence of the amount of CMPII(III,R•) formed during the reaction. All of the kinetic data were fitted to Scheme 3, in which CC(II) reacts only with the radical site. All of the species in Scheme III were assumed to be in the transient protein conformation in which the radical on Trp-191 is stabilized, k_2 and k_3 were assumed to be large compared to k_1, and k_4 was assumed to be equal to k_1. The entire pH dependence of the kinetics could be explained by an increase in the ratio $K = k_2/k_3$ from 0.02 to 1.0 as the pH is decreased from 8 to 5. This mechanism suggests that the electron transfer pathway recently proposed by Pelletier and Kraut (1992) on the basis of the crystal structure of the yeast iso-1-cytochrome *c*–CcP complex could be used for reduction of both CMPI and CMPII. This pathway extends from the exposed heme methyl group CBC of cytochrome *c* through cytochrome *c* peroxidase residues Ala-194, Ala-193, and Gly-192 to the indole group of Trp-191, which is in van der Waals contact with the heme group.

However, the pH dependence of the stopped-flow kinetic data could also be adequately fitted by the independent sites model of Scheme 2 (Hahm et al., 1994). What is needed to distinguish between these mechanisms is a method to reduce the radical in CMPI more rapidly than the rate constant k_2 for conversion of CMPII(IV,R) to CMPII(III,R•). Geren et al. (1991) and Hahm et al. (1992) have recently developed a technique to measure rapid electron transfer within complexes between ruthenium-labeled horse and yeast cytochrome *c* derivatives and CMPI. All of the derivatives reduced the radical in CMPI at rates up to 55 000 s^{-1} at pH 7 in low ionic strength buffer. In the present paper we use this new ruthenium photoexcitation technique to study the conversion of CMPII(IV,R) to CMPII(III,R•) at low pH.

We have also found that mutation of CcP Met-230 to Ile dramatically decreases the rate of conversion of CMPII(IV,R) to CMPII((III,R•) and the rate of reduction of CMPII. The X-ray crystal structure of the CcP(MI,M230I) mutant was determined to a resolution of 2.2 Å and revealed that significant changes in structure were confined to the region of residue 230 itself, with no changes in the position of the indole side chain of Trp-191 or other residues close to the heme.

EXPERIMENTAL PROCEDURES

Materials. Horse cytochrome *c* (type VI) and yeast iso-1-cytochrome *c* (type VIIIB) were purchased from Sigma Chemical Co. Yeast iso-1-cytochrome *c* (yCC) was treated with dithiothreitol to reduce any disulfide cross-linked dimers, passed through a Bio-Gel P2 column to remove excess reagent, and stored in the reduced form under nitrogen. Cytochrome *c* derivatives labeled at single lysine amino groups with (dicarboxybipyridine)bis(bipyridine)ruthenium(II) (Ru-CC) were prepared as described by Pan et al. (1988), Durham et al. (1989), and Geren et al. (1991). CcP(MI) and the mutant CcP(MI,M230I) were prepared as described by Fishel et al. (1987, 1991) and Miller et al. (1988).

Flash Photolysis Studies Using Ru-CC Derivatives. Laser flash photolysis studies of the reactions between Ru-CC derivatives and cytochrome *c* peroxidase were carried out as described by Geren et al. (1991) and Hahm et al. (1992). Mixtures of Ru-CC and cytochrome *c* peroxidase CMPI were prepared in buffers containing sodium acetate and sodium phosphate at the indicated ionic strength and pH, 1–10 mM aniline, and 0–500 mM sodium chloride. Aniline was present to reduce Ru(III) to Ru(II) and prevent the back-reaction. The rate constants were independent of the concentration of aniline. The kinetic transients were fitted to biexponential equations using the OLIS KINFIT program as described by Hahm et al. (1992).

Stopped-Flow Kinetics. Transient kinetic studies were carried out on a Durrum Model D-110 stopped-flow spectrophotometer using the protocols recently developed by Hahm et al. (1993, 1994). In protocol A, CC(II) was mixed with excess CMPI at high ionic strength to resolve the first electron transfer step in the reaction. The second-order rate constant k_a measured from 416-nm transients represents all reactions involving oxidation of CC(II) by CMPI. In protocol B, excess CC(II) was mixed with CMPI. The second-order rate constant k_b measured from the 434-nm transients represents all reactions involving reduction of the oxyferryl heme Fe(IV) by CC(II). The transients were fitted to the second-order equation:

$$\Delta A = 2\Delta\epsilon\left(b_0 - \frac{\exp[(b_0 - a_0)kt] - 1}{\exp[(b_0 - a_0)kt]/a_0 - 1/b_0}\right) \quad (1)$$

where b_0 = initial [CC(II)], a_0 = [CMPI], and $\Delta\epsilon$ is the difference extinction coefficient. The following difference extinction coefficients were used: CC(II) → CC(III), $\Delta\epsilon_{416} = -40$ mM^{-1} cm^{-1}, $\Delta\epsilon_{434} = 0$, $\Delta\epsilon_{550} = -18.6$ mM^{-1} cm^{-1}; CMPI → CMPII(IV,R), $\Delta\epsilon_{416} = -2$ mM^{-1} cm^{-1}, $\Delta\epsilon_{434} = +3$ mM^{-1} cm^{-1}; CMPII(IV,R) → CcP(III,R), $\Delta\epsilon_{416} = -13$ mM^{-1} cm^{-1}, $\Delta\epsilon_{434} = -27$ mM^{-1} cm^{-1} (Hahm et al., 1994; Coulson et al., 1971; Ho et al., 1983). The 416- and 434-nm transients obtained with both protocols were also fitted to Scheme 3 using numerical integration methods (Hahm et al., 1994).

X-ray Crystal Structure Analysis. Single crystals for X-ray diffraction studies were obtained under conditions similar to those used for other CcP(MI) mutants (Wang et al., 1990). Single large crystals were obtained in 2–5 days at room temperature by seeding with small crystals. The M230I crystals were isomorphous with the original wild-type crystal within experimental error (space group $P2_12_12_1$; $a = 105.0$ Å, $b = 74.2$ Å, $c = 45.4$ Å, $\alpha = \beta = \gamma = 90°$). X-ray data were collected on a Xuong–Hamlin multiwire area detector (Xuong et al., 1985) at room temperature using 0.13-deg increments/

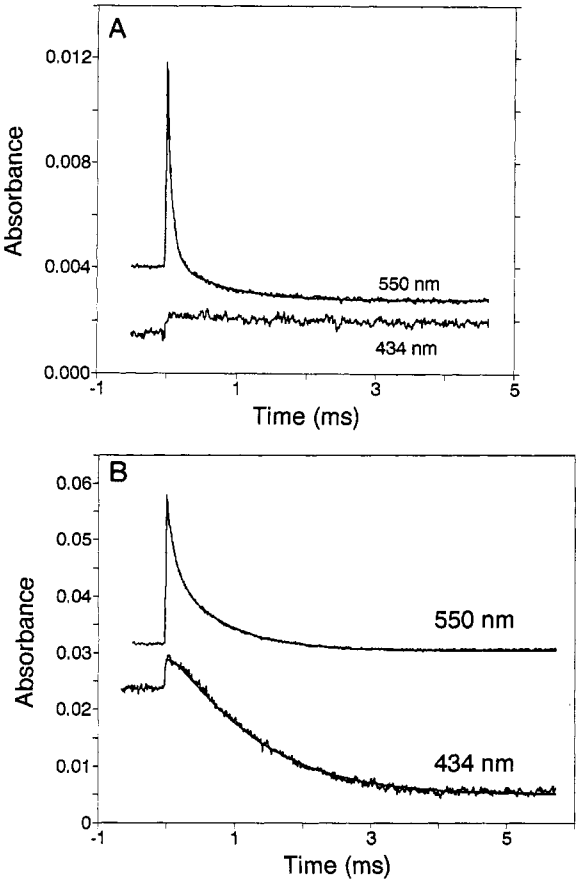

FIGURE 1: Photoinduced electron transfer from Ru-72-CC to CcP(MI) CMPI. (A) pH 7. The solution contained 5 μM Ru-72-CC and 5 μM CMPI in 2 mM sodium phosphate, pH 7, and 10 mM aniline. The reaction was initiated by a single 450-nm laser flash. The smooth line is the best fit to a biexponential with k_f = 14 000 s^{-1}, k_s = 1500 s^{-1}, and f = 0.7. (B) pH 5. The solution contained 3 μM Ru-72-CC and 3 μM CMPI in 1 mM sodium phosphate, 2 mM sodium acetate, pH 5, and 10 mM aniline. The smooth lines are the best fits of Scheme 4 to the 550- and 434-nm transients with k_f = 9000 s^{-1}, k_s = 1300 s^{-1}, f = 0.5, k' = 1100 s^{-1}, and K = 1.2.

frame and 20-s exposures/frame. A total of 18 426 unique reflections were collected, representing 99% of all unique data to 2.2 Å. The final R_{sym} was 5.5%.

The initial model of the M230I mutant was constructed by examining the difference Fourier map, F_o(M230I) − F_o(parent), displayed by the computer graphics program TOM (version 3.2b with modification by S. Dempsey at UCSD; Cambillau & Horjales, 1987; Jones, 1978) using an Iris 4D/340 VGX graphics system. The PROLSQ programs were used for least-squares refinement. A final R factor of 16.7% was obtained for data to 2.2-Å resolution. The rms deviations of bond lengths and bond angles from their dictionary values were 0.019 Å and 2.7°, respectively. Crystallographic coordinates have been submitted to the Brookhaven Data Bank under the name 1CEP.

RESULTS

Photoinduced Electron Transfer between Ru-CC Derivatives and CMPI. Flash photolysis of a solution containing 5 μM Ru-72-CC[1] and 5 μM CcP(MI) CMPI in 2 mM sodium phosphate, pH 7, resulted in rapid electron transfer from Ru(II*) to the heme Fe(III) of Ru-72-CC, followed by biphasic electron transfer from Fe(II) to CMPI (Figure 1A). The two phases had rate constants of k_f = 14 000 s^{-1} and k_s = 1500 s^{-1}, and the fraction of the fast phase was f = 0.7. No absorbance decrease was observed at 434 nm (a CC isobestic) (Figure 1A), indicating that both phases involved electron transfer to the radical in CMPI, as previously reported by Hahm et al. (1992) for the reaction between Ru-72-CC and wild-type yeast CMPI at pH 7. The small increase in absorbance at 434 nm is consistent with reduction of the radical, since Coulson et al. (1971) reported $\Delta\epsilon_{434}$ = +3 mM^{-1} cm^{-1} for reduction of the radical in CMPI. The kinetics were independent of protein concentration above 3 μM, indicating that both phases were due to intracomplex electron transfer. Hahm et al. (1992) have suggested that the fast phase is due to reduction of the radical by Ru-72-CC bound in the active site, while the slow phase is due to reorientation of Ru-72-CC from an inactive site to the active site. When the reaction between Ru-72-CC and CMPI was studied at pH 5, a 434-nm transient was observed, indicating reduction of the Fe^{IV}=O center (Figure 1B). The 434-nm transient clearly had a lag phase and was slower than the 550-nm transient, indicating that reduction of Fe^{IV}=O occurred after reduction of the radical in CMPI. Both the 434- and 550-nm transients were fitted to the kinetic equations for the mechanism given in Scheme 4. The best fit to the 550-nm transient was obtained with k_f = 9000 s^{-1}, k_s = 1300 s^{-1}, and f = 0.5 (Figure 1B). The conversion of CMPII(IV,R) to CMPII(III,R•) is not detected at 550 nm, since these species have nearly the same absorbance at this wavelength (Coulson et al., 1971). The last step in Scheme 4 is measured from the 434-nm transient, since 434 nm is an isobestic for cytochrome c. Using the values of k_f and k_s from the 550-nm transient, the 434-nm transient was fit with $k' = k_2 + k_3$ = 1100 ± 150 s^{-1}. The time dependence of the 434-nm transient simulated by Scheme 4 depends only on $k' = k_2 + k_3$ and is independent of the ratio k_2/k_3. The relative amplitudes of the 550- and 434-nm transients indicated that 1.4 μM Ru-72-CC was oxidized and 0.77 μM Fe^{IV}=O was reduced during the reaction, indicating that the ratio K = CMPII(III,R•)/CMPII(IV,R) = 1.2 ± 0.2. If a rapid equilibrium is assumed for the last step of Scheme 4, then $K = k_2/k_3$. With this assumption, the 434-nm transient was fitted with k_2 = 600 ± 100 s^{-1} and k_3 = 500 ± 100 s^{-1}. The values of k', k_2, and k_3 were independent of protein concentration and, also, the amount of CMPI reduced by Ru-72-CC, which could be controlled by the intensity of the laser flash. As the ionic strength was increased, the values of k_f and k_s decreased due to complex dissociation, but k' remained constant up to at least 50 mM ionic strength, where reduction of the radical became rate-limiting.

Scheme 4

$$\text{CC(II)–CMPI(IV, R•)}_f \xrightarrow{k_f} \text{CC(III)–CMPII(IV, R)}$$

$$\text{CC(II)–CMPI(IV, R•)}_s \xrightarrow{k_s} \text{CC(III)–CMPII(IV, R)}$$

$$\text{CC(III)–CMPII(IV, R)} \underset{k_3}{\overset{k_2}{\rightleftharpoons}} \text{CC(III)–CMPII(III, R•)}$$

The experiments were repeated with Ru-27-CC, which has larger rate constants for intracomplex electron transfer to CMPI than Ru-72-CC. Hahm et al. (1992) previously reported that there was no 434-nm transient absorbance change for the reaction of Ru-27-CC with CMPI at pH 7, indicating no formation of CMPII(III,R•). However, at pH 5, a 434-nm transient was observed, indicating reduction of Fe^{IV}=O (Figure 2). The 550-nm transient was fitted to Scheme 4 with k_f = 43 000 s^{-1}, k_s = 1600 s^{-1}, and f = 0.77. The 434-nm transient was fitted with k' = 1100 ± 150 s^{-1}. The amplitudes of the 550- and 434-nm transients indicated that 0.6 μM

[1] Abbreviations: yCC, yeast iso-1-cytochrome c; hCC, horse cytochrome c; Ru-72-CC, bis(bipyridine)(4,4′-dicarboxybipyridine-Lys-72-cytochrome c)ruthenium(II).

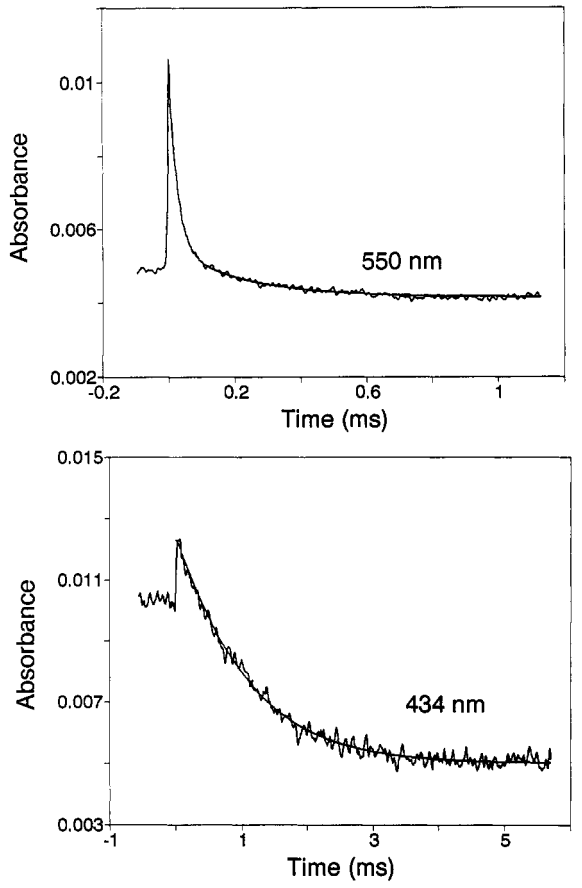

FIGURE 2: Photoinduced electron transfer from Ru-27 to CMPI at pH 5. The solutions contained 3 μM Ru-27-CC and 3 μM CMPI in 1 mM sodium phosphate, 2 mM sodium acetate, pH 5, and 10 mM aniline. The smooth lines are the best fits of Scheme 4 to the 550- and 434-nm transients with k_f = 43 000 s^{-1}, k_s = 1600 s^{-1}, f = 0.77, k' = 1100 s^{-1}, and K = 1.3.

Table 1: Photoinduced Electron Transfer between Ru-CC Derivatives and CcP(MI) CMPI[a]

pH	k_f	k_s	f	k'	K	k_2	k_3
			Ru-72-CC				
5.0	9 000	1300	0.5	1100	1.2	600	500
6.0	16 000	2000	0.7	550	0.4	150	400
7.0	14 000	1500	0.7		≤0.15		
			Ru-27-CC				
5.0	43 000	1600	0.8	1100	1.3	600	500
5.4	35 000	1600	0.9	600	0.8	270	330

[a] The solutions contained 3 μM Ru-CC and 3 μM CcP(MI) CMPI in 1 mM sodium phosphate and 5 mM sodium acetate at the indicated pH and 10 mM aniline. The 550- and 434-nm transients were fitted to Scheme 4 as described in the text. The rate constants are in units of s^{-1}. The error is ±15%.

CC(II) was oxidized and 0.34 μM Fe^{IV}=O was reduced, giving K = 1.3 ± 0.2. With the rapid equilibrium assumption, k_2 = 600 ± 100 s^{-1} and k_3 = 500 ± 100 s^{-1}. The values of k', k_2, and k_3 were independent of protein concentration and the amount of CMPI reduced, and of ionic strength up to at least 50 mM. Experiments with yeast iso-1-Ru-102-CC were also consistent with the same k', k_2, and k_3 values (data not shown).

Experiments were also carried out at higher pH values (Table 1). The value of k' was 600 s^{-1} for Ru-27-CC at pH 5.4, and 550 s^{-1} for Ru-72-CC at pH 6. The ratio K was significantly smaller at the higher pH values, decreasing to 0.4 ± 0.2 at pH 6. The values of k', K, k_2, and k_3 are given in Table 1. No significant 434-nm transients were observed at pH values higher than 6, indicating that the value of K was smaller than 0.15.

Table 2: Intracomplex Electron Transfer between Ru-CC Derivatives and CcP(MI,M230I)[a]

	Ru-13-CC			Ru-27-CC			Ru-72-CC		
mutant	k_f	k_s	f	k_f	k_s	f	k_f	k_s	f
CcP(MI)	6.6	2.3	0.6	39	1.2	0.8	12	2.2	0.7
M230I	12	0.4	0.8	48	0.2	0.7	20	0.5	0.6

[a] The solutions contained 5 μM Ru-CC and 6–15 μM CcP(MI,M230I) in 2 mM sodium phosphate, pH 6.4, and 10 mM aniline at 25 °C. The rate constants were measured from the 550-nm transient following a single laser flash as described in Figure 1. The rate constants are in units of 10^3 s^{-1}. The error limits are ±15%.

Photoinduced Electron Transfer between Ru-CC Derivatives and CcP(MI,M230I). The CMPI form of CcP(MI,M230I) was not very stable at pH 7, so the kinetic studies were carried out at pH 6.4, where CMPI was stable for at least 5 min. Photoexcitation of a solution containing 5 μM Ru-27-CC and 6 μM CcP(MI,M230I) CMPI resulted in biphasic electron transfer from the Ru-27-CC heme Fe(II) to CMPI. No 434-nm transient absorbance change was observed, indicating that both phases were due to electron transfer to the radical in CMPI. The rate constants of the fast and slow phases were 48 000 and 230 s^{-1}, respectively, compared to 39 000 and 1200 s^{-1} for CcP(MI) CMPI (Table 2). These rate constants were independent of the concentration of CMPI as long as it was greater than that of Ru-CC, indicating that both phases were due to intracomplex electron transfer. The kinetics of the reactions of CcP(MI,M230I) with Ru-13-CC and Ru-72-CC were also studied at pH 6.4 (Table 2). In all cases, the fast phase rate constant for CcP(MI,M230I) was larger than that of CcP(MI), while the slow phase rate constant was smaller.

Ionic strength had a significant effect on the kinetics of reactions between the Ru-CC derivatives and both CcP(MI) and CcP(MI,M230I). As the ionic strength was increased from 2 mM sodium phosphate, pH 6.4, the fast phase rate constant and amplitude decreased and the slow phase rate constant and amplitude increased until a single phase was observed at about 20 mM ionic strength. This suggests that increasing the ionic strength leads to rapid exchange of Ru-CC between the active and inactive binding sites (Hahm et al., 1992). At 20 mM ionic strength, the observed rate constant k_{obs} had a hyperbolic dependence on CMPI concentration which was fit by equation:

$$k_{obs} = k_{et}[C]/(K_d + [C]) \quad (2)$$

k_{et} is the intracomplex rate constant from CC to CMPI, K_d is a dissociation constant, and [C] is the concentration of CMPI. The best fit for the reaction between Ru-72-CC and CcP(MI) CMPI at 20 mM ionic strength, pH 6.4, was k_{et} = 6100 s^{-1}, and K_d = 7 μM. For the reaction between Ru-72-CC and CcP(MI,M230I), the values were k_{et} = 4400 s^{-1} and K_d = 7 μM.

The reactions between Ru-CC derivatives and CcP(MI,M230I) were also studied at low pH, where reduction of the oxyferryl heme Fe(IV) was observed for CcP(MI). No 434-nm transient absorbance changes were detected for the reactions of either Ru-72-CC or Ru-27-CC with CcP(MI,M230I) at pH values from 5 to 6.4. This indicates that the reduction of Fe(IV) was less than 10% that of the radical.

Stopped-Flow Studies of the Reactions between Yeast and Horse Cytochrome c and CcP(MI) and CcP(MI,M230I) CMPI. The protocols developed by Hahm et al. (1993, 1994) were used to study the pH dependence of the reaction between yeast iso-1-cytochrome c (yCC) and CcP(MI) CMPI. In protocol A, yCC(II) was mixed with excess CMPI to measure

Table 3: pH Dependence of the Reaction between yCC(II) and CMPI[a]

pH	k_a	k_b	k_1	K_e
6.0	150	40	140	0.45
7.0	150	20	140	0.19
8.0	140	13	140	0.12

[a] The second-order rate constants k_a and k_b for the reaction of yCC(II) were measured using protocols A and B in buffer containing 5 mM sodium phosphate, 5 mM sodium acetate, and NaCl added to a total ionic strength of 400 mM. The transients were fitted to Scheme 3 assuming that $k_4 = k_1$, k_2 and k_3 are large compared to k_1, and $K_e = k_2/k_3$. The second-order rate constants are all given in units of 10^6 M^{-1} s^{-1}. The error in each parameter is ±20%.

Table 4: Second-Order Rate Constants for the Reaction of CcP(MI,M230I) CMPI with hCC(II) and yCC(II)[a]

mutant	k_a, horse	k_b, horse	k_a, yeast	k_b, yeast
CcP(MI)	1.5×10^8	3.0×10^7	1.5×10^8	3.5×10^7
M230I	1.3×10^8	2.5×10^6	1.5×10^8	2.5×10^6

[a] The reactions with hCC were carried out in 2 mM sodium phosphate, 2 mM sodium acetate, and 100 mM NaCl, pH 6, and the reactions with yCC were carried out in 5 mM sodium acetate, 5 mM sodium phosphate, and 390 mM NaCl, pH 6, 25 °C. The second-order rate constants are given in units of M^{-1} s^{-1}, and the error is ±20%.

the first electron transfer step. Much higher ionic strength was needed to resolve the reaction in the stopped-flow instrument than was the case for hCC (Hahm et al., 1994). The second-order rate constant k_a measured at a constant ionic strength of 400 mM remained nearly constant at 1.5×10^8 M^{-1} s^{-1} from pH 6 to 8 (Table 3). No absorbance change was detected at 434 nm at pH 7–8. However, at lower pH a small 434-nm transient with decreasing absorbance was observed, indicating partial reduction of Fe^{IV}=O. The rate constant of the 434-nm transient was the same as that of the 416-nm transient, indicating rapid equilibrium between the two forms of CMPII as shown in Scheme 1. At pH 6 the relative amplitudes of the 416- and 434-nm transients indicated that the ratio K = CMPII(III,R•)/CMPII(IV,R) = 0.5 ± 0.2 after equilibrium was reached. The value of K was ≤0.15 at pH 7 and 8.

The second-order rate constant k_b measured from the 434-nm transient using excess yCC(II) (protocol B) increased from 1.3×10^7 M^{-1} s^{-1} to 4.0×10^7 M^{-1} s^{-1} as the pH was decreased from 8.0 to 6.0 (Table 3). This is much smaller than the 18-fold increase in k_b for hCC observed over the same pH range (Hahm et al., 1994). This difference might be related to the much higher ionic strength needed for the yCC studies than for the hCC studies (110 mM). The complete kinetic data including both the 416- and 434-nm transients from pH 6 to 9 were fitted to Scheme 3 using numerical integration techniques as described by Hahm et al. (1994). The equilibration between the two forms of CMPII was assumed to be rapid compared to the reduction steps, consistent with the fact that the rate of the 434-nm transient is the same as that of the 416-nm transient at pH 6 under protocol A. In addition, the rate constant k_4 was assumed to be equal to k_1. The rate constant k_1 remained relatively constant at (1.4 ± 0.2) × 10^8 M^{-1} s^{-1} from pH 6 to pH 8, while $K_e = k_2/k_3$ decreased from 0.45 to 0.12 (Table 3).

The reactions between horse and yeast cytochrome *c* and CcP(MI,M230I) were studied at pH 6 using stopped-flow spectroscopy. For the reaction involving hCC in 2 mM sodium phosphate, pH 6, and 100 mM NaCl, the rate constant k_a measured using protocol A was 1.3×10^8 M^{-1} s^{-1}, compared to 1.5×10^8 M^{-1} s^{-1} for the CcP(MI) control (Table 4). However, no absorbance change was detected at 434 nm,

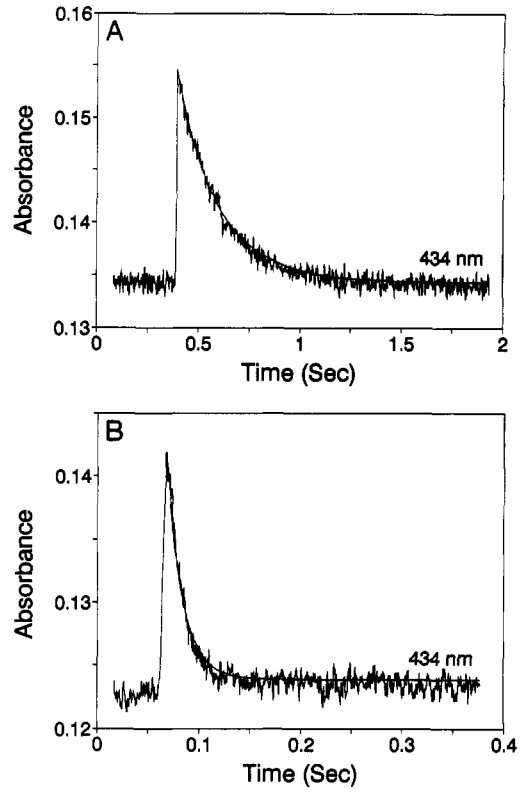

FIGURE 3: Reaction between native hCC(II) and CcP(MI,M230I) CMPI at pH 6 in the stopped-flow spectrophotometer. (A) The reaction mixture contained 3 μM hCC(II) and 0.6 μM CcP(MI,M230I) in 2 mM sodium phosphate, pH 6, and 100 mM NaCl. The solid line is the best fit of eq 1 to the 434-nm transient with $k_b = 2.5 \times 10^6$ M^{-1} s^{-1}. (B) The reaction mixture contained 3 μM hCC(II) and 0.6 μM wild-type CcP(MI) CMPI in the same buffer as in (A). The solid line is the best fit of eq 1 to the 434-nm transient with $k_b = 3.0 \times 10^7$ M^{-1} s^{-1}.

indicating no reduction of Fe^{IV} and $K < 0.1$. By comparison, a 434-nm transient was observed in the reaction of hCC with CcP(MI) CMPI at pH 6, indicating partial reduction of Fe^{IV}, with K = 0.4 ± 0.2 (Hahm et al., 1994). The rate constant k_b measured using protocol B was only (2.5 ± 0.7) × 10^6 M^{-1} s^{-1}, 12-fold less than the value for CcP(MI) (Figure 3, Table 4). Similar results were obtained for the reaction of yCC with CcP(MI,M230I) at pH 6 and 400 mM ionic strength (Table 4). The rate constant k_a was nearly the same as that of CcP(MI), and no 434-nm transient was observed using protocol A. The rate constant k_b was 14-fold less than that for CcP(MI) (Table 4).

X-ray Crystallography of CcP(MI,M230I). Figure 4 shows a difference electron density map, F_o(M230I) − F_o(CcP(MI)), superimposed on a model of the CcP(MI) structure in the region of the mutation. The strongest features of the map are near the side chain of residue 230 itself. A large peak of negative density (−5σ) is centered over the SD and CE atoms of the Met-230 side chain. A positive peak of electron density (5σ), representing the CG2 group of Ile-230, also flanks this side chain.

As suggested by the difference Fourier map, significant changes in the refined structure of M230I were confined to the region of the mutation. The refined structure of M230I in this region is compared with that of the CcP(MI) parent in Figure 5. As shown in Figure 5, the substitution of Ile for Met-230 causes a small adjustment of the peptide chain at position 230. A rotation of the 230 residue by ~15° around the Cα–Cβ bond was observed, causing a shift of 0.96 Å in the position of CG of residue 230. The rotation is probably caused by the introduction of a branched side chain at position

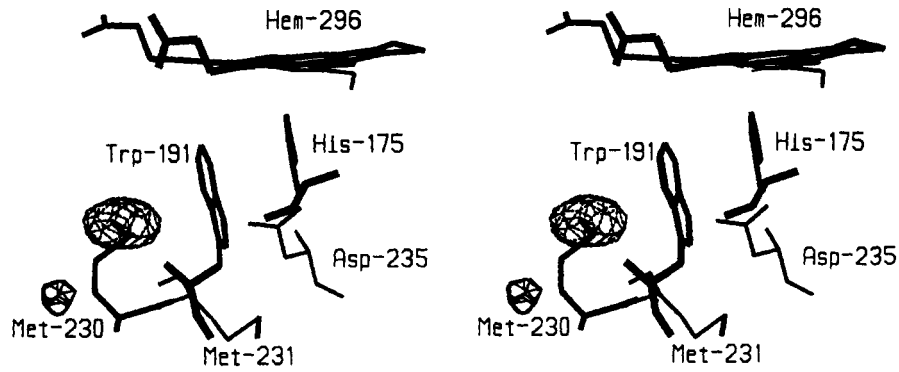

FIGURE 4: CcP(MI,M230I) minus CcP(MI) difference Fourier map contoured at $\pm 5\sigma$. Dashed contour lines represent negative difference density; solid lines represent positive difference density. The difference map is superimposed on a model of the CcP(MI) structure in the region of the mutation.

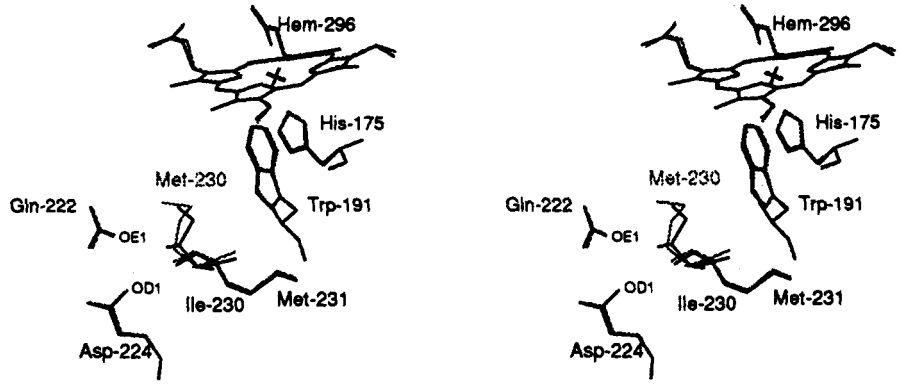

FIGURE 5: Superposition of refined structures of CcP(MI,M230I) (solid lines) and CcP(MI) (dashed lines).

230, as it prevents close contacts of the CG2 methyl of Ile-230 with OE1 of Gln-222 and OD1 of Asp-224. Despite the change in the orientation of the side chain at 230, the position of the indole ring of Trp-191 was within experimental error the same as its position in the CcP(MI) parent (Figure 5). Likewise, there were no changes in the positions of the side chains of Asp-235 or His-175 on the proximal side of the heme.

Small changes in the solvent water were also introduced during the refinement. Highly disordered water molecules ($B > 120$) were removed, and a single new water molecule (HOH 753) was added near the distal face of the heme. The new water molecule is within hydrogen bonding distance of O of the carbonyl group of Pro-145, HOH 724, and HOH 445, with distances ranging from 2.70 to 3.01 Å.

DISCUSSION

Flash Photolysis Experiments Indicate Sequential Reduction of CMPI. Previous studies have indicated that one-electron reduction of CMPI(IV,R$^{\bullet}$) by cytochrome *c* produces a mixture of CMPII(IV,R) and CMPII(III,R$^{\bullet}$) (Coulson et al., 1971). The relative proportion of the two species is pH-dependent, with the proportion of CMPII(III,R$^{\bullet}$) produced decreasing from 56% at pH 5.0 to less than 12% at pH 7.0. An important question that was not resolved by the prior studies is whether the relative proportion of these two species is determined by reduction of CMPI at one site, followed by a rearrangement between the two forms of CMPII (e.g., Schemes 1 and 3), or by independent reduction at the two sites (e.g., Scheme 2). The experiments reported here demonstrate that initial reduction converts CMPI(IV,R$^{\bullet}$) to CMPII(IV,R), followed by an intramolecular electron transfer reaction. This constitutes clear evidence in favor of a mechanism where a single site is reduced, followed by redistribution of the oxidizing equivalent between the oxyferryl heme and the Trp-191 radical.

The photolysis experiments described here involve reduction of the Trp-191 radical at a rate that is much faster than the rate of intramolecular electron transfer. The fast, biphasic oxidation of cytochrome c coupled to the reduction of the compound I radical is indicated by the change in absorbance at 550 nm and the absence of a change at 434 nm, the cytochrome *c* isobestic. As expected for an intermolecular electron transfer reaction, the rate of this process is dependent upon ionic strength as well as the location of the Ru label on cytochrome *c*. The subsequent reduction of Fe^{IV} by the indole group on Trp-191 is indicated by the change in absorbance at 434 nm with no corresponding change at 550 nm. The lag phase evident for the 434-nm transient further indicates that it is the second process of a sequential mechanism. As expected for an internal electron transfer reaction, the rate of this reaction was unaffected by protein concentration, ionic strength, or the location of the Ru label on cytochrome *c*. These results are inconsistent with an independent sites mechanism such as that shown in Scheme 2.

It is important to note that the present results also rule out an alternative mechanism involving disproportionation of the CMPII(IV,R) intermediate. Although 2 molecules of CMPII(IV,R) could theoretically react to form CMPI(IV,R$^{\bullet}$)- and CcP(III,R), the values of k', k_2, and k_3 were independent of CMPII(IV,R) concentration, thus eliminating any second-order process from consideration. Ho et al. (1983, 1984) have also presented evidence that disproportionation of CMPII-(IV,R) does not occur.

The mechanisms proposed in Schemes 3 and 4 require the existence of the intermediate CMPII(III,R$^{\bullet}$) in rapid equilibrium with CMPII(IV,R). While no such intermediate has been directly characterized, the existence of CMPII(III,R$^{\bullet}$) was inferred by Coulson et al. (1971) on the basis of EPR and spectrophotometric studies. These experiments indicated that Fe^{IV}=O and the Trp-191 radical are reduced equally during

Table 5: pH Dependence of the Ratio K of the Two Forms of CMPII Generated by One-Electron Reduction of CMPI[a]

pH	method A	method B	method C
5.0	1.2	1.1	1.2
5.4		0.8	0.8
6.0	0.54	0.4	0.4
7.0	0.15	≤0.15	≤0.15
8.0	0.0	≤0.05	≤0.15

[a] The ratio K = CMPII(III,R•)/CMPII(IV,R) was measured by equilibrium titration with ferrocyanide [A; data of Coulson et al. (1971)], stopped-flow reaction with hCC [B; data of Hahm et al. (1994)], and Ru-CC photoreduction (C; present studies). The buffers used were 0.1 M potassium phosphate in A, 8 mM sodium phosphate, 5 mM sodium acetate, and NaCl to a total ionic strength of 110 mM in B, and 1 mM sodium phosphate and 5 mM sodium acetate in C, all at 25 °C.

the reaction of CMPI with one reducing equivalent of cytochrome *c* or ferrocyanide at pH 5.0. While the existence of CCPII(III,R•) has long been assumed, a rapid equilibrium between CMPII(IV,R) and CMPII(III,R•) has not been demonstrated. Indeed, Ho et al. (1983, 1984) found that the reaction of ferrous CcP with hydrogen peroxide resulted in formation of the stable form of CMPII, CMPII(IV,R)$_B$, with no significant amounts of CMPII(III,R•) at pH 7.0 and room temperature, or at pH 5.0 under cryogenic conditions. Moreover, the reported rate constants for conversion of the stable form of CMPII(IV,R)$_B$ to CMP(III,R•) at pH 7 or pH 7.5 (Ho et al., 1983, 1984; Summers & Erman, 1988) are too slow to account for the results obtained here and by Coulson et al. (1971). To resolve this apparent discrepancy, Ho et al. (1983) proposed that CMPI(IV,R•) has a protein conformation that stabilizes the radical on Trp-191 by lowering its redox potential. One-electron reduction of CMPI results in formation of CMPII(IV,R) that retains the transient protein conformation stabilizing the radical. A competition then occurs between intramolecular electron transfer converting the transient form of CMPII(IV,R) to CMPII(III,R•), and relaxation of CMPII(IV,R) to the stable form, CMPII(IV,R)$_B$, in which Trp-191 has a high redox potential and is not readily oxidized. In such a mechanism, K would be a constant determined by the ratio of the rate constants for these competing processes rather than a true equilibrium constant. The present results do not discriminate between these two possibilities.

A Strong Correlation Exists between the Rates of Intramolecular Electron Transfer and Reduction of CMPII. Regardless of whether the relative proportion of CMPII(IV,R) and CMPII(III,R•) is determined by a kinetic or an equilibrium process, the present results show that the value of K for intramolecular electron transfer is identical to the values of K obtained from stopped-flow studies of bimolecular CMPI and CMPII reduction (Hahm et al., 1994), and from reductive titrations of CMPI (Coulson et al., 1971; Table 5). Furthermore, the pH dependence of K is also essentially the same with all three techniques (Table 5). Thus, the kinetic process resolved by the Ru-CC photoexcitation technique leads to the same final products observed in the stopped-flow and equilibrium titration studies. This observation provides strong evidence that the rate of CMPII reduction by cytochrome *c* is a function of the rate of intramolecular electron transfer from Trp-191 to the Fe^{IV}=O center.

The correlation between intramolecular electron transfer and CMPII reduction is further emphasized by the flash photolysis and stopped-flow results obtained using CcP(MI,M230I). The photolysis experiments showed that while the Met-230 → Ile mutation had little effect on the biphasic reduction of the CMPI Trp radical by Ru-CC, the subsequent intramolecular reduction of Fe^{IV}=O could not be detected. The failure to detect intramolecular reduction of the Fe^{IV}=O center by Trp-191 in the M230I enzyme correlates with a significant decrease in the rate of CMPII reduction. Stopped-flow experiments employing hCC and yCC showed that although the bimolecular reduction of the Trp-191 radical was similar for CcP(MI,M230I) and the CcP(MI) parent enzyme, the rate of CMPII reduction was decreased 12-fold in the M230I enzyme relative to the CcP(MI) parent. Depending upon the mechanism of electron transfer between Trp-191 and the Fe^{IV}=O center, the results suggest that the M230I mutation either shifts the equilibrium toward formation of CMPII(IV,R) and away from CMPII(III,R•) or decreases the rate of electron transfer from Trp-191 to the oxyferryl center.

The effect of the M230I mutation can be simply explained as a perturbation of the redox potential of Trp-191. The sulfur atoms of Met-230 and Met-231 are approximately 4.5 Å from the indole side chain of Trp-191. The presence of two sulfur atoms in close proximity to the indole ring is suggestive of a functional role for these atoms in stabilizing the indole radical and/or increasing the rate of electron transfer from Trp-191 to the heme (Edwards et al., 1987; Fishel et al., 1991). A structural basis for the effects of the M230I mutation is ruled out by the crystal structure of the M230I enzyme. Perturbations of the M230I crystal structure are minor and are confined to the immediate region of the mutation. The positions of the Trp-191, Asp-235, and His-175 side chains of the M230I mutant enzyme are within error the same as their positions in the parent CcP(MI).

Together, the results demonstrate a strong correlation between the rate of reduction of CMPII measured by stopped-flow techniques and the rate of intramolecular reduction of the oxyferryl center measured by flash photolysis. The results therefore provide strong support for a mechanism that proceeds through sequential reduction, reoxidation, and reduction of Trp-191 as the predominant mechanism for electron transfer under the present conditions. The mechanism may involve an equilibrium (e.g., Scheme 3) or a kinetic partitioning of oxidizing equivalents between the oxyferryl center and Trp-191, as suggested by Ho et al. (1983). A sequential mechanism utilizing the Trp-191 radical as an intermediate would also explain the effect of the W191F mutation on electron transfer rates. Previous studies have shown that the rate of reduction of the oxyferryl center of W191F is decreased at least 1000-fold relative to the CcP(MI) parent, although the electronic properties of the oxyferryl center of the W191F mutant appear to be similar to those of the parent (Mauro et al., 1988; Wang et al., 1990). The requirement for the Trp-191 indole ring in the reduction of Fe^{IV}=O by cytochrome *c* would explain the dramatic effect of this mutation on electron transfer rates.

Relationship between Transient and Steady-State Experiments. The present results provide strong evidence that the reduction of CMPI occurs through sequential one-electron transfer reactions to an indole radical at Trp-191. An important question is whether reduction of Fe^{IV}=O always involves reduction of the radical as in Scheme 3, or whether direct reduction of Fe^{IV}=O could occur, through either a Pelletier–Kraut pathway or a different pathway. A critical issue in evaluating this possibility is whether or not the intra- and intermolecular electron transfer rates are competent to support the overall kinetic scheme. The rate constants k_2 and k_3 determined from flash photolysis are large enough to fit the stopped-flow results obtained at pH 5 and 6 using Scheme 3. However, k_2 and k_3 could not be measured directly at higher pH, and so it is not possible to tell whether the conversion

of CMPII(IV,R) to CMP(III,R•) is fast enough to account for k_b, the experimentally determined rate of reduction of Fe^{IV}=O. Thus, the present data are internally consistent where both electron transfer rates can be measured.

It is also of considerable importance to evaluate whether or not the electron transfer rates determined here are sufficient to account for steady-state rates reported by others. For example, the optimum turnover number for the reaction of yCC with CcP at pH 6 under steady-state conditions is 1300 s^{-1} (Kang et al., 1977). This is considerably larger than the value of k_2 measured from Ru-CC studies at pH 6, suggesting that other mechanisms may contribute to the steady-state rate. One possibility is that yCC could reduce Fe^{IV}=O using the Kraut–Pelletier pathway in a superexchange mechanism that does not require actual oxidation and reduction of Trp-191. This mechanism is supported by the finding of Geren et al. (1991) that Ru-102-yCC reduces Fe^{IV}=O in the stable form of $CMPII(IV,R)_B$ with an intracomplex rate constant of 1000 s^{-1} at pH 7. The conversion of $CMPII(IV,R)_B$ to CMPII(III,R•) is too slow to account for this rate constant (Ho et al., 1983). An alternative possibility is that, at the high excess concentrations of yCC used in the steady-state assay, yCC could bind to a second low-affinity site on CMPII and directly reduce Fe^{IV}. The presence of a second binding site is supported by the report of Stemp and Hoffman (1993) that electron transfer from yCC to Zn-porphyrin CcP is fast only when 2 mol of yCC are bound/mol of CcP. In a complementary study, Zhou and Hoffman (1993) found that Zn-CC binds to a second site on the Zn-CC/CcP complex that allows rapid electron transfer to the heme Fe(III). Steady-state and stopped-flow data on the reaction between excess CC and CMPI also suggest that direct reduction of Fe^{IV}=O might occur at low ionic strength (Summers & Erman, 1988; Erman et al., 1991; Nuevo et al., 1993). Yi et al. (1994) recently found that the rate constant for dissociation of the 1:1 yCC/CcP product complex was 180 s^{-1} at low ionic strength and increased with increasing concentrations of solution yCC. Since the dissociation of the product complex was much slower than the turnover number, they proposed that the interaction of substrate yCC(II) at a second site could promote dissociation of product yCC(III) from the high-affinity site.

Rate Constant for Intramolecular Electron Transfer in CMPII. An interesting question raised by the present studies is why the rate of intramolecular electron transfer associated with the reaction CMPII(IV,R) → CMPII(III,R•) is so slow, <1000 s^{-1}. X-ray crystallography has shown that the indole ring of Trp-191 is close to the heme group and that Asp-235 forms hydrogen bonds to both the indole ring and the imidazolate of His-175, which is the proximal iron ligand (Finzel et al., 1984; Edwards et al., 1987) (Figure 4). Indeed, Goodin and McRee (1993) have recently suggested that this Asp–His–Fe triad might help align the indole ring of Trp-191 for efficient coupling between the free radical and the heme group. Houseman et al. (1993) have recently modeled the anomalous EPR spectrum of CMPI by a weak exchange interaction between the $S = 1$ Fe^{IV}=O center and the radical on the indole group of Trp-191. The slow rate of electron transfer associated with conversion of CMPII(IV,R) to CMPII(III,R•) could be due to a large reorganization energy. Since the driving force for the reaction is expected to be close to zero at pH 5, this would lead to a slow rate. Alternatively, the conversion could be accompanied by a rate-limiting protein conformational change.

REFERENCES

Cambillau, C., & Horjales, E. (1987) *J. Bol. Graphics. 5*, 174–177.

Coulson, A. F. W., Erman, J. E., & Yonetani, T. (1971) *J. Biol. Chem. 246*, 917–924.

Durham, B., Pan, L. P., Long, J., & Millett, F. (1989) *Biochemistry 28*, 8659–8665.

Edwards, S. L., Xuong, N. H., Hamlin, R. C., & Kraut, J. (1987) *Biochemistry 26*, 1503–1511.

Erman, J. E., Vitello, L. B., Mauro, J. B., & Kraut, J. (1989) *Biochemistry 28*, 7992–7995.

Erman, J. E., Kang, D. S., Kim, K. L., Summers, F. E., Mathis, A. L., & Vitello, L. B. (1991) *Mol. Cryst. Liq. Cryst. 194*, 253–258.

Finzel, B. C., Poulos, T. L., & Kraut, J. (1984) *J. Biol. Chem. 259*, 13027–13036.

Fishel, L. A., Villafranca, J. E., Mauro, J. M., & Kraut, J. (1987) *Biochemistry 26*, 351–360.

Fishel, L. A., Farnum, M. F., Mauro, J. M., Miller, M. A., Kraut, J., Liu, Y., Tan, X., & Scholes, C. P. (1991) *Biochemistry 30*, 1986–1996.

Geren, L. M., Hahm, S., Durham, B., & Millett, F. (1991) *Biochemistry 30*, 9450–9457.

Goodin, D. B., & McRee, D. E. (1993) *Biochemistry 32*, 3313–3324.

Hahm, S., Durham, B., & Millett, F. (1992) *Biochemistry 31*, 3472–3477.

Hahm, S., Geren, L., Durham, B., & Millett, F. (1993) *J. Am. Chem. Soc. 115*, 3372–3373.

Hahm, S., Miller, M. A., Geren, L., Kraut, J., Durham, B., & Millett, F. (1994) *Biochemistry 33*, 1473–1480.

Ho, P. S., Hoffman, B. M., Kang, C. H., & Margoliash, E. (1983) *J. Biol. Chem. 258*, 4356–4363.

Ho, P. S., Hoffman, B. M., Solomon, N., Kang, C. H., & Margoliash, E. (1984) *Biocehmistry 23*, 4122–4128.

Houseman, A. L. P., Doan, P. E., Goodin, D. B., & Hoffman, B. M. (1993) *Biochemistry 32*, 4430–4443.

Jones, T. A. (1978) *J. Appl. Crystallogr. 11*, 268–272.

Kang, C. H., Ferguson-Miller, S., & Margoliash, E. (1977) *J. Biol. Chem. 252*, 919–926.

Kim, K. L., Kang, D. S., Vitello, L. B., & Erman, J. E. (1990) *Biochemistry 29*, 9150–9159.

Mauro, J. M., Fishel, L. A., Hazzard, J. T., Meyer, T. E., Tollin, G., Cusanovich, M. A., & Kraut, J. (1988) *Biochemistry 27*, 6243–6256.

Miller, M. A., Hazzard, J. T., Mauro, J. M., Edwards, S. L., Simons, P. D., Tollin, G., & Kraut, J. (1988) *Biochemistry 27*, 9081–9088.

Nuevo, M. R., Chu, H.-H., Vitello, L. B., & Erman, J. E. (1993) *J. Am. Chem. Soc. 115*, 5873–5874.

Pan, L. P., Durham, B., Wolinska, J., & Millett, F. (1988) *Biochemistry 27*, 7180–7184.

Pelletier, H., & Kraut, J. (1992) *Science 258* 1748–1755.

Sivaraja, M., Goodin, D. B., Smith, M., & Hoffman, B. M. (1989) *Science 245*, 738–740.

Stemp, E. D. A., & Hoffman, B. M. (1993) *Biochemistry 32*, 10848–10865.

Summers, F., E., & Erman, J. E. (1988) *J. Biol. Chem. 263*, 14267–14275.

Wang, J., Mauro, J. M., Edwards, S. L., Oatley, S. J., Fishel, L. A., Ashford, V. A., Xuong, N. H., & Kraut, J. (1990) *Biochemistry 29*, 7160–7173.

Xuong, N.-H., Nielsen, C. P., Hamlin, R., & Anderson, D. H. (1985) *J. Appl. Crystallogr. 18*, 342–350.

Yi, Q., Erman, J. E., & Satterlee, J. D. (1994) *J. Am. Chem. Soc. 116*, 1981–1987.

Yonetani, T. (1965) *J. Biol. Chem. 240*, 4509–4514.

Zhou, J. S., & Hoffman, B. M. (1993) *J. Am. Chem. Soc. 115*, 11008–11009.